

The Cavity in the Inner HD 100546 Disk: The potential for spectral imaging with TPF-Coronagraph

C.A. Grady (Eureka Scientific and GSFC)
and
Bruce Woodgate (NASA's GSFC)

Abstract

The TPF coronagraph, currently slated to launch in 2014, will have a factor of nearly 3 times the spatial resolution of HST, and if equipped with a true multi-spectral imaging capability, such as can be provided by a coronagraphic integral field spectrometer, can be a superb platform for studying the transition from protoplanetary disks dominated by accretion onto the star to young planetary systems at the onset of the era of Heavy Bombardment. Multi-spectral imaging from such a platform can resolve the dust sublimation region around A stars to $d=25$ pc, the region interior to the "snow line", where chemistry can occur, out to the location of the nearest star-forming regions ($d=150$ pc), and will provide 4-5 resolution elements across disks comparable in size to the proto-Solar nebula at $d=450$ pc. HST observations of one Herbig Be star, HD 100546, indicate that spectral imaging extending down to Lyman α offers the potential to image centrally cleared zones, to detect peri-center asymmetries in the distribution of remnant dust and gas, to map stellar wind geometries, and to map the distribution of molecular and ionic gas in the planetary region. Direct detection of chromospheric and transition region emission associated with brown dwarfs can also be used to distinguish between extra-solar giant planets and stellar/ substellar body binary systems.

I. Introduction

To understand the diversity of known planetary systems, we must understand how they arise, and what factors in the protoplanetary disk+star evolution of the system produce Solar Systems like our own. The final phases in the evolution of the protoplanetary disk appear to be critical not only in establishing for how long a star will be classified as a Herbig Ae or

classical T Tauri star (Haisch et al. 2001), but also in establishing the architecture of the mature planetary system. TPF has the potential not only to discover terrestrial planets around nearby stars, but also to tease out the typical history of planetary systems during the early portions of the Era of Heavy Bombardment.

II. Protoplanetary Disk Studies To Date

Meeus et al. (2001) found that the spectral energy distributions (SEDs) of Herbig Ae disks could be sorted into two broad groups: those with SEDs which could be fit as power-laws, consistent with disks which passively reprocess the stellar light, and those which had additional emission in the 40-160 μm range. Dullemond & Dominik (2004a,b) and Meeus et al. (2001) suggested that the power-law only disks are the result of geometrical shadowing of the outer disk by material in a hot dust ring at the dust sublimation temperature (0.3-0.5 AU), while the power-law + excess flux SEDs result when the disk is unshadowed and has a flared photosurface. Acke & van den Ancker (2004) and Acke et al. (2004) have found that the shadowed disks have shallower sub-mm indices which they interpreted as indicating larger average grain sizes.

In parallel with these efforts, coronagraphic imaging with HST has shown that there is a wide diversity in disk sizes, and surface brightnesses in both Herbig Ae and classical T Tauri disks, at distances $r \geq 0.5''$ (50-70 AU) from the stars. In some cases the disk non-detections appear to be associated with geometrically small disks (Grady et al. 2004a), while others are known to have large disks imaged in the millimeter (Mannings & Sargent 1997, 2000; Mannings, Koerner, & Sargent 1997; Simon et al. 2001). Analysis of the Herbig Ae data indicates that rather than correlating with disk mass, sub-mm spectral index, or the strength and/or shape of the 10 μm silicate emission, the disk surface brightness correlates with the strength of the PAH emission (Grady et al. 2004b, see fig. 1). To radiate in the mid-IR bands, PAHs require transient absorption of FUV photons at levels well above the fluxes provided by the ambient interstellar radiation field. For the nearby Herbig Ae/Be stars studied by HST/STIS and ISO the only source of additional FUV flux is the star itself. Therefore, the PAH emission associated with the Herbig Ae/Be star traces material which is sufficiently far above the disk mid-plane that it has a direct line of sight to the star rather than material in the disk mid-plane.

STIS also observed a millimeter-selected sample of classical T Tauri stars, with disks spanning a similar size and surface brightness range to the Herbig Ae stars. While PAH detections are atypical of mid-IR T Tauri data, presumably due to a lower FUV flux than for the Herbig Ae stars, T Tauri stars excite conspicuous fluorescent H_2 emission in the FUV (Herczeg et al. 2002). The available data for the classical T Tauri stars with known, large disks suggests that the disk optical surface brightness correlates with the relative strength of the spatially extended fluorescent H_2 emission (fig. 2). For the known, large disks, the STIS coronagraphic non-detections are preferentially associated among the older sample members with millimeter data indicating the presence of large grains.

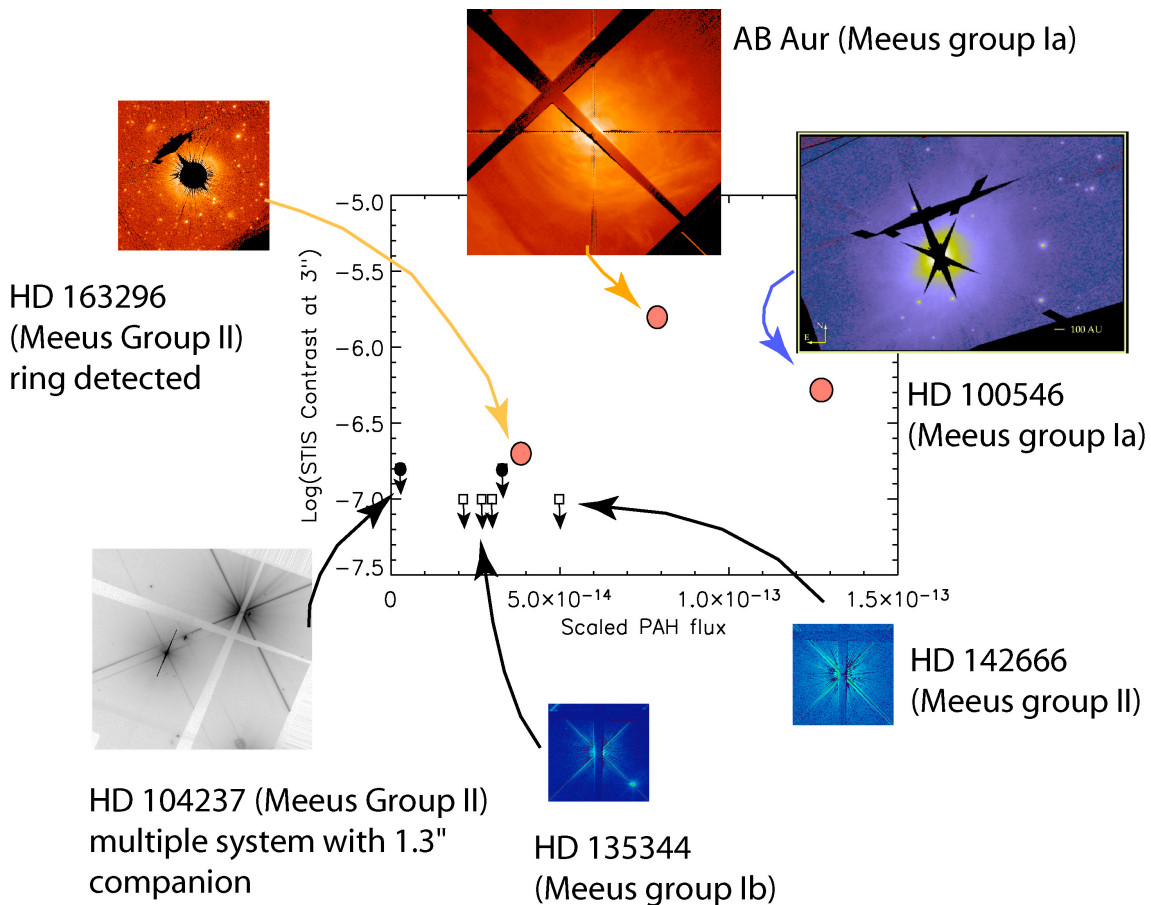


Fig. 1: The optical surface brightness of Herbig Ae star disks as a function of the PAH emission strength, scaled to $d=100$ pc for the stars with data in Acke & van den Ancker (2004).

The PAH and H₂ data suggest that the surface brightness of the large disks which were not detected by STIS is within 1-2 orders of magnitude of the current upper limits (Grady et al. 2003; Schneider et al. 2003). Improvements in coronagraph performance at this level, due to suppression of the stellar PSF, are in the range of designs which could be implemented on a telescope like HST within 3 years. More importantly, what these data indicate is that detection of young exo-planets or substellar companions to young stars must occur against a bright, nebulous background.

III. Finding the Young Planetary Systems

The presence of bright line or reflection nebulosity, while normally not thought of as an advantage in planet searches, can be exploited to separate the accreting protoplanetary systems from those which have some degree of central clearing, but which are not yet as cleared as β Pic or AU Mic (Kalas et al. 2004). Analysis of the mid-IR SEDs have suggested that 3-10 AU scale central cavities are present around HD 100546 (Bouwman et al. 2003), and the T Tauri stars GM Aur, DM Tau, Lk Ca 15, and TW Hya (Bergin et al. 2004). Demonstrating that a cavity is a physically cleared zone should ideally be done using a variety of diagnostics including the presence of features in the IR SED, a low current accretion rate (low UV/FUV excess), the absence of microjet activity near the star, and imaging of a region exhibiting low reflection nebulosity and low molecular gas emission relative to more distant portions of the circumstellar disk. While such data could, in principal, be obtained through the combination of multi-spectral imaging and integrated-light spectroscopy, an alternate, and more efficient, approach is to make use of spectral resolution in tandem with high angular resolution and high contrast. Such a study was carried out under the auspices of the STIS GTO program for some of the nearest Herbig Ae stars (Grady et al. 2004c).

With radial extents of 0.03-0.1" at d=100 pc, the cavities are inaccessible to HST coronagraphic imaging. However, the relevant spatial scales were sampled by STIS long-slit spectroscopy. When carried out in deep photospheric absorption profiles from the primary star spectrum, the photospheric direct, scattered, and diffracted light is suppressed by factors of 10^{3-4} relative to observations where the star is bright. Use of this "spectroscopic null" of the star therefore achieves contrasts approaching that of coronagraphic imaging, but with a factor of 10 improvement in proximity to the star (fig. 3). Coupling observations in such spectroscopic nulls with

imaging spectroscopy improves the contrast for detection of emission line nebulosity, either due to outflows (Devine et al. 2004; Grady et al. 2004a), or due to fluorescent emission from molecules such as H_2 by not only suppressing the stellar contribution, but also suppressing the reflection nebulosity (Grady et al. 2004b).

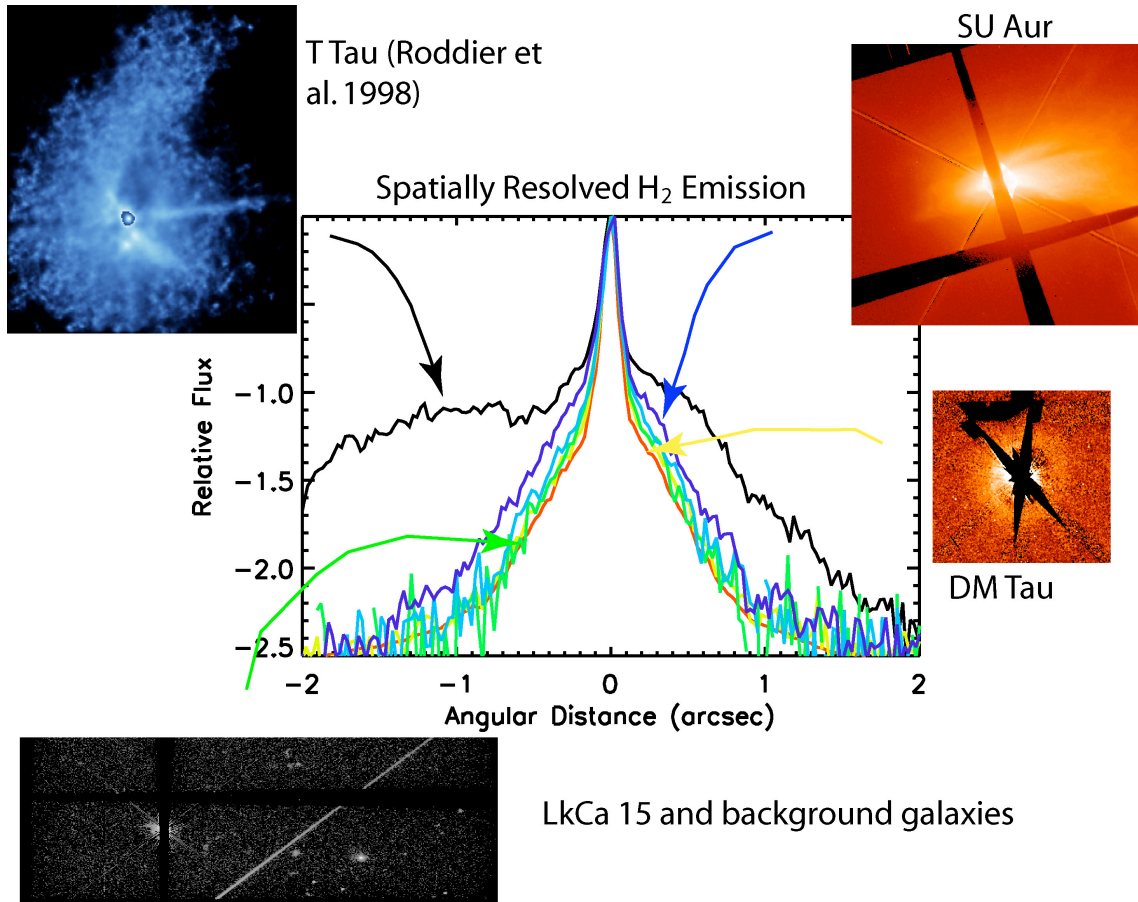


Fig. 2: A number of classical T Tauri stars have both optical imagery (direct and coronagraphic) and UV spatially resolved spectroscopy. Spatial profiles derived from the STIS G140L spectra in the 1400-1500 Å region are shown above for several classical T Tauri stars. The surface brightness of the nebulosity appears to correlate with the excess light seen in the H_2 transitions within 140 AU of the star. Black: T Tau, Blue: SU Aur, Yellow: DM Tau, Green, Lk Ca 15, Orange: PSF template star GD 71.

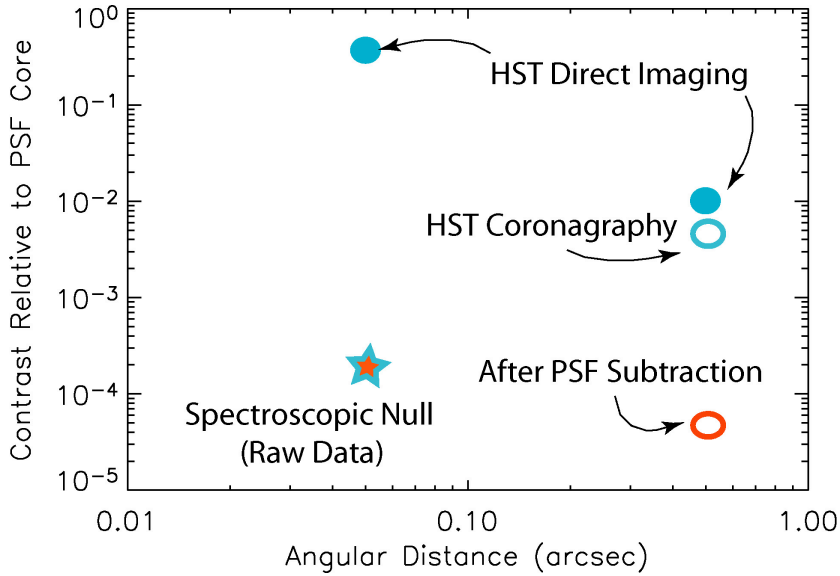


Fig. 3: Comparison of contrasts achieved via HST coronagraphy (STIS) and using conventional long-slit spectroscopy in deep photospheric absorption lines. Further improvement in contrast are feasible via subtraction of high S/N PSF data.

IV. Imaging Nearby Protoplanetary Disks with Central Cavities

Mid-IR studies of the IR spectral energy distributions of PMS stars have indicated that there are both Herbig Ae and Classical T Tauri stars with evidence for central cavities in the dust and gas disks (Bouwman et al. 2004; Bergin et al. 2004). One such object is HD 100546 (KR Mus, B9.5Ve, $d=103.6$ pc, $t \geq 10$ Myr, van den Ancker et al. 1998) which has been coronagraphically imaged by HST (Augereau et al. 2001; Grady et al. 2001; Ardila et al. 2004), as well as spectrally imaged at Ly α (Grady et al. 2004). The Ly α data reveal extended reflection nebulosity, as well as emission in Ly α , N I, and H₂ transitions pumped by Ly α (fig. 4). The H₂ emission is not detected in the point source spectrum, and the surface brightness of the reflection nebulosity is not as centrally peaked as would be expected for material extending in to the dust sublimation radius at 0.3-0.5 AU. More detailed analysis has revealed that the spatially extended nebulosity is offset from the star by 5 AU along the system minor axis. After correcting for the r^{-2} fall off in the stellar radiation field, there is an $r \approx 13$ AU central cavity (fig. 5). The STIS and ACS data (Ardila et al. 2004) also do not reveal any indication of a bipolar microjet, while the STIS and FUSE data (Deleuil et al. 2004) suggest that the current accretion rate is at least an order of magnitude lower than for younger Herbig Ae stars such as HD 163296 (Devine et al. 2000) or HD 104237 (Grady et al. 2004a).

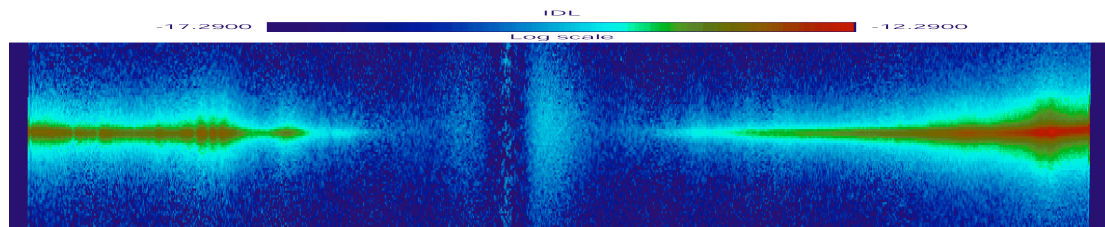


Fig. 4. The inner ± 100 AU along the system minor axis for HD 100546. The spectrum is dispersed from 1190-1245 \AA horizontally, while the vertical axis images the disk along a $52'' \times 0.2''$ slit. Spatially extended Ly α , N I, and H₂ emission are visible in addition to reflection nebulosity (from Grady et al. 2004b).

Scattering asymmetries would be expected to be present along the system minor axis, and should not be seen along the system major axis. Radiation pressure blow-out of small grains and Poynting-Robertson drag will act symmetrically upon dust in the inner disk and should not produce an asymmetric cavity. Dynamical sculpting of the disk by either a bound companion or by an unbound object are the only mechanisms proposed to date capable of producing peri-center asymmetries in the dust and gas distribution. The effects of external perturbers have been invoked to account for tidal truncation of disks, and to produce the structure seen in the HD 141569 A disk (Augereau & Papaloizou 2004), while the effect of planets has been invoked to account for structure in debris disks such as HR 4796 A (Wyatt et al. 1999). HD 100546 has no known companions external to the disk (Grady et al. 2001), and has the x-ray luminosity consistent with the presence of at most 1 early M star within $0.1''$ of the Herbig Ae star (Feigelson et al. 2003). Such a body would be detected via its diffraction spikes in the STIS coronagraphic imagery. The non-detection of chromospheric and transition region emission from a second source (with distinctive line profiles) in the STIS long slit spectra places an upper limit in spectral type of M5.5V. At the age of HD 100546, this suggests that any bound companion within the disk must be no more massive than a brown dwarf. Bouwman et al. (2004) place a lower limit on a single body of $5.5 M_{\text{Jup}}$ on the mass of such a companion from the size of the Hill sphere required to maintain the IR SED. Direct detection (Tsuboi et al. 2003) via detection of chromospheric emission will require suppression of the stellar PSF by a factor of 60-70 in Si III compared to STIS's default performance. Inspection of the available G140L spectral imagery of the Bergin et al. (2004) classical T Tauri stars, while demonstrating the presence of extended

nebulousity on scales larger than $0.1''$, does not unambiguously resolve the predicted 3-6 AU cavities. At distances of 140 pc, a larger aperture is clearly required.

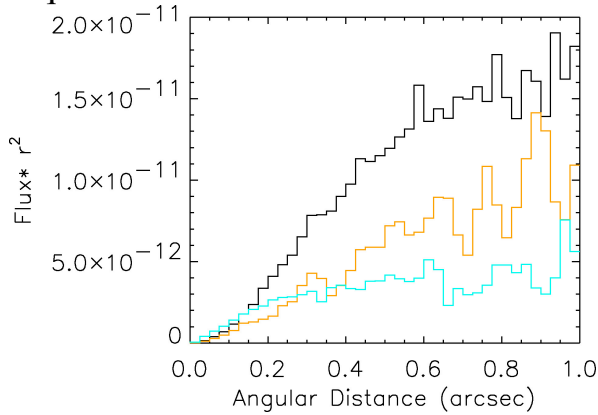


Fig. 5. After correcting for illumination effects, the spatial profiles for Ly α (black), the continuum (blue) and H₂ emission (orange) show a deficit of scatterers similar to that seen in β Pic within $0.1''$ (10 AU) of the star.

V. UV Spectral Imaging with TPF-Coronagraph

While early designs for TPF-Coronagraph favored silver-overcoated primary and secondary mirrors, recent analysis shows that aluminum-overcoated optics for the first two mirrors can achieve both the desired off-angle response for the coronagraph, low scattering needed for coronagraphic work, and a UV spectral response (Bowers, priv. comm.). As a result, it is now feasible to consider what could be done with a spectral imaging capability for TPF extending into the vacuum UV. Either integral field or long slit spectrographs may be used for UV spectroscopy. For detection and characterization of material around a star, and substellar companions, the STIS data demonstrate that moderate spectral resolution ($R=10,000$ for point sources) is sufficient to separate reflection nebulousity from emission line features, and to permit characterization of the emission line nebulousity. High dynamic range in a single observation is essential: our STIS Herbig Ae star imaging spectra have contrast ranges of ≥ 3500 . The current STIS/HST data are PSF-limited for the T Tauri stars, with HD 100546 less affected due to use of the deep null afforded by Ly α .

These observations did not reach the limit of spectral imaging for HST. STIS FUV MAMA observations were normally taken in a mode (repeller-on) which collects photons scattered by the web between microchannels. Higher

angular resolution data were feasible for STIS, but were not implemented in flight, since the factor of 4 suppression in the PSF halo at $r \geq 0.07''$ was accompanied by a 60% loss of signal. With the advent of higher QE UV detectors (Norton, et al. 2003), this loss of throughput is not a serious problem for future instrumentation. Similar suppression of the wings of the PSF can be achieved for future instrumentation via use of electron bombarded CCDs, with higher QE photocathodes compensating for any signal loss, or by use of a commandable repeller for micro-channel detectors. When coupled with the PSF gains, at fixed angular distance from the star, by going to a larger, diffraction-limited telescope, such as TPF-Coronagraph, the contrast gain due to use of a spectroscopic null, reduced in-detector scatter of photons, and a larger telescope is $\approx 10^6$. If we assume that the Ly α emission from young brown dwarfs scales with their x-ray luminosity, this is a factor of 10 gain above that needed to directly detect 10 Myr brown dwarfs similar to TWA 5B within 0.1" of the primary in raw spectral imagery. To be suitable for high contrast coronagraphic imagery, TPF-Coronagraph will also need to suppress the telescope scattered light contribution to the PSF. If gains of 10^{3-4} relative to HST are achieved, well below the requirements for direct exoplanet detection, UV spectral imaging will achieve contrasts needed to detect accretion onto young exo-Jupiters at 100 pc in the immediate vicinity of A-star primaries.

VI. Conclusions

Combining spectral imaging, high contrast imaging will permit substellar companion and exoplanet detection with achievable apertures even in the presence of significant exo-zodiacal light if the wavelength coverage extends to portions of the spectrum where the primary star photosphere is dark.

This study made use of data obtained as part of HST-GTO-8891., HST-GTO-8474, and HST-GO-9136. Support for the STIS IDT was provided by NASA Guaranteed Time Observer funding to the STIS Science Team in response to NASA A/O OSSA -4-84 through the HST Project at GSFC. CAG was supported through NASA PO 70789-G to Eureka Scientific. Analysis facilities were provided by the Laboratory for Astronomy & Solar Physics at NASA's GSFC.

VII. References:

- Acke, B. & van den Ancker, M.E. 2004, A&A (in press).
- Acke, B. et al. 2004 A&A 422, 621.
- Ardila, D. et al. 2004, ApJ (in preparation).

Augereau, J.C. et al. 2001, A&A 365, 78.
Augereau, J.C.& Papaloizou, J.C.B. 2004, A&A 414, 1153.
Bergin, E. A. et al. 2004, ApJ (in press).
Bouwman, J. et al. 2003, A&A 401, 577.
Deleuil, M. et al. 2004, A&A 418, 577.
Devine, D. et al. 2000, ApJ. 542, L115.
Dullemond, C.P. & Dominik, C. 2004a, A&A 417, 159.
Dullemond, C.P.& Dominik, C. 2004b, A&A 421, 1075.
Feigelson, E. et al. 2003, ApJ 599, 1207.
Grady et al. 2001, AJ 122, 3396.
Grady et al. 2003, PASP, 115, 1036.
Grady, C. et al. 2004a, ApJ 608, 809.
Grady, C. et al. 2004b, ApJ (in press).
Grady, C. et al. 2004c, ApJ (in preparation).
Haisch, K. E. Jr. et al. 2001 ApJ 553 L153.
Herczeg, G. et al. 2002, ApJ 572, 310.
Kalas, P. et al. 2004, Sci, 303, 1990.
Mannings, V. et al. 1997, Nature, 388, 555.
Mannings, V., & Sargent, A.I. 1997, ApJ 490, 792.
Mannings, V. & Sargent, A.I. 2000, ApJ 529, 391.
Meeus, G. et al. 2001, A&A 365, 476.
Norton, T. et al. 2003, SPIE, 5164, 155.
Schneider, G. et al. 2003
Simon, M. et al. 2000, ApJ 545, 1034.
Tsuboi, Y. et al. 2003, ApJ 587, L51.
Wyatt, M.C. 2003, ApJ 598, 1321.